(12) INTERNATIONAL APPLICATION PUBLISHED UNDER THE PATENT COOPERATION TREATY (PCT)

(19) World Intellectual Property Organization
International Bureau

(43) International Publication Date
02 November 2017 (02.11.2017)

WIPO | PCT

(10) International Publication Number
WO 2017/188559 A1

(51) International Patent Classification:
G06T 11/00 (2006.01) *G06T 3/00* (2006.01)

(21) International Application Number:
PCT/KR2017/000506

(22) International Filing Date:
13 January 2017 (13.01.2017)

(25) Filing Language: English

(26) Publication Language: English

(30) Priority Data:
10-2016-0053493 29 April 2016 (29.04.2016) KR

(71) Applicant: **IM TECHNOLOGY.CO.,LTD** [KR/KR]; (Gireum-dong, Hyunyang Building), 2F West, 6 Gireum-ro 6, Seongbuk-gu, Seoul 02725 (KR).

(72) Inventor: **JUN, Kyung Taek**; (Namyang-dong, Weed Park apartments) 99 Gayang-ro, Seongsan-gu, Changwon-si, Gyeongsangnam-do 51480 (KR).

(74) Agent: **LEE & KO IP**; Hanjin Building 25F, 63 Namdaemun-ro, Jung-gu, Seoul 04532 (KR).

(81) Designated States *(unless otherwise indicated, for every kind of national protection available)*: AE, AG, AL, AM, AO, AT, AU, AZ, BA, BB, BG, BH, BN, BR, BW, BY, BZ, CA, CH, CL, CN, CO, CR, CU, CZ, DE, DJ, DK, DM, DO, DZ, EC, EE, EG, ES, FI, GB, GD, GE, GH, GM, GT, HN, HR, HU, ID, IL, IN, IR, IS, JP, KE, KG, KH, KN, KP, KR, KW, KZ, LA, LC, LK, LR, LS, LU, LY, MA, MD, ME, MG, MK, MN, MW, MX, MY, MZ, NA, NG, NI, NO, NZ, OM, PA, PE, PG, PH, PL, PT, QA, RO, RS, RU, RW, SA, SC, SD, SE, SG, SK, SL, SM, ST, SV, SY, TH, TJ, TM, TN, TR, TT, TZ, UA, UG, US, UZ, VC, VN, ZA, ZM, ZW.

(84) Designated States *(unless otherwise indicated, for every kind of regional protection available)*: ARIPO (BW, GH, GM, KE, LR, LS, MW, MZ, NA, RW, SD, SL, ST, SZ, TZ, UG, ZM, ZW), Eurasian (AM, AZ, BY, KG, KZ, RU, TJ, TM), European (AL, AT, BE, BG, CH, CY, CZ, DE, DK, EE, ES, FI, FR, GB, GR, HR, HU, IE, IS, IT, LT, LU, LV, MC, MK, MT, NL, NO, PL, PT, RO, RS, SE, SI, SK, SM, TR), OAPI (BF, BJ, CF, CG, CI, CM, GA, GN, GQ, GW, KM, ML, MR, NE, SN, TD, TG).

Published:
— *with international search report (Art. 21(3))*

(54) Title: METHOD OF IMAGE RECONSTRUCTION IN COMPUTED TOMOGRAPHY

FIG. 1

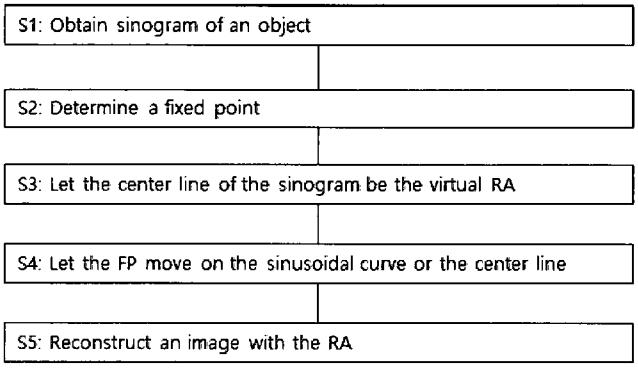

(57) Abstract: Since X-ray tomography is now widely adopted in many different areas, it becomes more crucial to find a robust routine of handling tomographic data to get quality reconstructed images. Though there are several existing techniques, it seems helpful to have a more automated method to remove the possible errors that hinder clearer image reconstruction. Here, we proposed an alternative method and new algorithm using the sinogram and the fixed point. A new physical concept of Center of Attenuation (CA) was also introduced to figure out how this fixed point is applied to the image reconstruction with errors we further categorized.

WO 2017/188559 A1

DESCRIPTION

Invention Title: Method of Image Reconstruction in Computed Tomography

【Technical Field】

The present invention relates to a method of image reconstruction and, more particularly, to a method of image reconstruction in computed tomography.

【Background Art】

Nowadays X-ray tomography is considered more than essential in various fields, and combined with advanced X-ray sources, it provides us with more sophisticated scientific insights. As Wang *et al.* "A high-throughput x-ray microtomography system at the Advanced Photon Source. *Rev. Sci. Instrum.* 72, 2062-2068 (2001) once argued, it is desirable to achieve an automated data processing with minimum human interaction due to the demand of high-throughput experiments. Given the fact that we only get the 2D projections from the x-ray penetration to form the internal 3D structure of a sample, a number of scientists have shared their insights to get rid of impairing effects in getting a quality reconstruction, translation and tilting errors, for example. They have focused on the determination of the center of rotation (CoR), and there are mainly three families of methods. The first category uses pairs of projection images taken from the reverse viewing angles (at 0-180 degrees). They perform the image registration of these pairs to calculate the offset of CoR. This method is often considered efficient, however, Vo, N. T., Drakopoulos, M., Atwood, R. C. & Reinhard, C. "Reliable method for calculating the center of rotation in parallel-beam tomography. *Opt. Express,* 22, 19078 (2014)" argued that it is not feasible especially when the projections have low contrasts or the optics system have fixed defects. The second method evaluates the projection image from the reconstruction using a parameter to measure the quality of image reconstruction and to calibrate the relative offset of the rotation axis (Gursoy, D., De Carlo, F., Xiao, X. & Jacobsen, C. TomoPy: a framework for the analysis of synchrotron tomographic data. *J. Synchrotron Rad.* 21,

1188-1193 (2014)). This technique is widely used and has its own strength in terms of using all the available information, but it is often time-consuming and inapplicable for the reconstruction with artifacts. The last one considered the center-of-mass (CM)(Donath, T., Beckmann, F. & Schreyer, A. Automated determination of the center of rotation in tomography data. *J. Opt. Soc. Am. A,* 23, 1048-1057 (2006)). To make it work, the sample should be within the field of view, which is not always possible.

【Disclosure】

【Technical Problem】

Even with these numerous efforts to minimize and correct the systemic defects, not all the errors are perfectly corrected and the process is usually too time consuming and laborious. Also, most error corrections were done only for a small amount of error.

Hence it is always useful to figure out a new method and algorithm to correct the flawed information to obtain a better quality image reconstruction.

The object of the present invention is to provide for an improved image reconstruction.

【Technical Solution】

In this article we propose an alternative approach to remove the errors, specifically translation and tilt errors by using the sinogram and the fixed point. Wherein, fixed point is defined as the point in space that can be discriminated or calculated by analysis of a projection image set. Fixed point is the point in space that can be discriminated or calculated by analysis of a projection image set. The real RA is located on the center line of the sinusoidal trajectory of the FP. Furthermore, we did not seek to determine the CoR; instead, we aligned the vertical center line of projection to the CoR to make it like a virtual RA, which was enabled by our algorithm.

We can estimate the real RA via the center line of the sinusoidal trajectory of the FP, as follows:

S1: Obtain sinogram of an object

S2: Determine a fixed point

S3: Estimate the RA via the center line of the sinusoidal trajectory of the FP

S4: Reconstruct an image with the RA

or

S1: Obtain sinogram of an object

S2: Determine a fixed point

S3: Estimate the RA via the center line of the sinusoidal trajectory of the FP

S4: Let the FP move on sinusoidal curve

S5: Reconstruct an image with the RA

In accordance with one aspect of the invention, a method of reconstructing an image in computed tomography is provided. The method comprises: obtaining a sinogram of an object; determining at least one fixed point of the object; letting the fixed point to be a virtual rotation axis such that the fixed point corresponds to a straight line across a center of the sinogram; calculating relative positions of points other than the fixed point of the object relative to the fixed point in the sinogram; and reconstructing an image based on a calcuation of the relative positions of the points.

In accordance with another aspect of the invention, a computer-implemented method for reconstructing an image in computed tomography is provided. The computer includes a processor, and the method comprises: obtaining, by the processor, a sinogram of an object; determining or receiving, by the processor, at least one fixed point of the object; translating, by the processor, the fixed point to be a virtual rotation axis such that the fixed point corresponds to a straight line across a center of the sinogram; calculating, by the processor, relative positions of points other than the fixed point of the object relative to the fixed point in the sinogram; and reconstructing, by the processor, an image based on a calculation of the relative positions of the points.

In accordance with another aspect of the invention, a non-transitory computer-readable medium having stored thereon computer-executable

instructions is provided. When executed by a computer, the computer-executable instructions cause the computer to: obtain a sinogram of an object; determine or receive at least one fixed point of the object; translate the fixed point to be a virtual rotation axis such that the fixed point corresponds to a straight line across a center of the sinogram; calculate relative positions of points other than the fixed point of the object relative to the fixed point in the sinogram; and reconstruct an image based on a calculation of the relative positions of the points.

In accordance with another aspect of the invention, a system for reconstructing an image in computed tomography is provided. The system comprises: a processor; an input coupled to the processor and configured to receive a parallel projection dataset; and a memory coupled to the processor. The memory includes computer-executable instructions that when executed by the processor cause the processor to: obtain a sinogram of an object; determine or receive at least one fixed point of the object; translate the fixed point to be a virtual rotation axis such that the fixed point corresponds to a straight line across a center of the sinogram; calculate relative positions of points other than the fixed point of the object relative to the fixed point in the sinogram; and reconstruct an image based on a calculation of the relative positions of the points.

Various other features and advantages will be made apparent from the following detailed description and the drawings.

【Description of Drawings】

Fig. 1 schematically shows a flow diagram of a method of image reconstruction in computed tomography according to an exemplary embodiment of the present invention.

Figs. 2a-2c are sinograms of specimen placed on several different part of the stage in which we marked the stage with the red dot at the bottom to indicate θ is zero degree.

Figs. 3a-3b are sinograms with the translation errors during the beam time.

Figs. 4a-4c are sinograms and reconstruction images of a layer of

Hanford soil in a polyether ether ketone(PEEK) column from National Synchrotron Light Source (NSLS) X2B beamline at Brookhaven National Laboratory (BNL).

Fig. 5 shows the sinogram and its reconstruction image with which we figured $\overrightarrow{P_{CA}}$ of each column in Fig. 3b sinogram and align them on the function $T_{50,30^\circ}$.

Figs. 6a-6c show analysis of a partial image of human lower jaw including the teeth.

Figs. 7a-7d show objects of prolate spheroid located on the rotating stage and their sinograms.

Figs. 8a-8c show the sinogram pattern of cylindrical specimen and the $\overrightarrow{CA}$ trajectory, depending on the tilt of the object or the RA.

Figs. 9a-9c show shadow changes depending on the location of a cylindrical specimen.

Fig. 10 shows a trajectory of a fixed point when there were several errors during beam time.

Figs. 11a-11b show the cases when the x-ray density of projection is changed during the beam time.

Figs. 12a-12c show optimized reconstruction images with various optimization methods.

Figs. 13a-13b show the common layer in the projections and the sinogram.

【Mode for Invention】

Before any embodiments of the invention are explained in detail, it is to be understood that the invention is not limited in its application to the details of construction and the arrangement of components set forth in the following description or illustrated in the following drawings. The invention is capable of other embodiments and of being practiced or of being carried out in various ways.

The relative position of an object in the real space and the sinograms in 2D

Fig. 1 schematically shows a flow diagram of a method of image reconstruction in computed tomography according to an exemplary embodiment of

the present invention.

As a first step, a sinogram of an object is obtained in step S1. A sinogram involves the information about a specific layer of an object and accumulates the projection shadows taken from each angle to build a reconstruction image of the layer. This sinogram will later be transformed into a reconstructed image through the inverse Radon transform or (Fast) Fourier transform with filters. Apparently, an errorless reconstructed image will be obtained only with an ideal sinogram or an ideal projection set, and a necessary condition for the ideal sinogram is that its pattern is changed sequentially following the projection angles.

When the location of an object is changed on the stage, the sinogram pattern will be also changed while the projection shadow from an angle remains the same. (1)

There might be slight differences in the projection shadow due to the limit of image digitalizing techniques; this can be approximated by a linear interpolation.

Where a projection shadow lies on the sinogram is closely related to where an object lies in the real space; this relationship should be first investigated before we further use sinograms for our analysis. The object on the rotating stage is known to rotate around the rotation axis (RA) and it means that any single point of the object has its own circular trajectory, which will be expressed as a sinusoidal function in the sinogram. The point on the RA will be the straight line across the center of the sinogram. Our hypothesis is that if we get the projection set of a specific object and if we know the ideal sinogram pattern of this object, we can modify the real sinogram pattern to meet the ideal one and consequently get the errorless reconstructed image. By modifying the sinogram, we can make the same effect as physically moving the object from where it was to the center on the stage, while the recorded image is preserved. This saves the present efforts of determining the CoR and setting the specimen on the RA, for the simple modification of sinogram will yield the same result.

The sinogram was constructed by a projection image of the circular

image specimen, a cross-sectional image of a cylinder in 2D. Fig. 2a shows when the specimen was located on the center of the stage. The stage rotated clockwise for the entire 180° or 360° , and the x-ray beam was fixed at θ=0. The sinogram pattern is linear in this case. One can easily spot the changes of the sinogram pattern when the cylinder was moved backward the parallel beam on the stage in Fig. 2b, and when it was moved to the right from the beam in Fig. 2c. The projection shadow from an angle remains the same, even when the specimen was moved to a different spot and had a different sinogram pattern.

Continuity & Discontinuity by an Object movement and a CT system Vibration

Assumed that the projection images are all clear, it is the translation error that we can first think of in the 2D space during the beam time. We categorized translation errors into two; the orthogonal translation and the parallel translation, which are the two elements in the basis that we decided to consider in this disclosure. By the orthogonal translation, we mean that the specimen is moved vertically from the parallel beam at the projection angle θ, while the parallel translation means that the specimen is moved toward to or away from the parallel beam. When the error occurs horizontally to the beam, the pattern of sinogram flows continuously showing no discontinuity in parallel translation (Fig. 3a). The graph which illustrates the value change of $f_n(t)$ to the angle, θ, doesn't have any discontinuity, either.

The error occurring vertically to the beam shows a definite cut-off point as the graph of Fig. 3b illustrates. In Fig. 3b, the error appeared when the parallel beam was shoot perpendicularly to the stage and the cut-off of the sinogram was reflected at the 90 degrees of θ. The error that arises when the specimen is moved perpendicularly to the beam is always reflected identically on the projection and the discontinuity of equal amount is also found in the sinogram. As a result, we can spot the exact point where the discontinuity happens and correct this error mathematically. It is the same in case of the graph with the value change of $f_n(t)$ to the angle, θ. The discontinuity is found at θ_e=90° , and the minimum is found at $t=49$ in the

graph.

If we have an orthogonal translation error in the e-th column, the correction process has to start from the point where the error occurred and the rest of sinogram has to be modified accordingly. Let us calculate how far the shadow has to be compensated in order to make this inaccurate sinogram an errorless, ideal one. V_n is the distance to which the n-th column has to be moved in the sinogram, and it is written as follows:

$$V_n = v * \cos(\theta_n - \theta_e), \quad n \geq e \ (\text{or } n < e)$$

θ_n indicates the angle of n-th column and θ_e is the angle at which the orthogonal translation error occurred in the sinogram. v is the distance that the object is vertically moved to, and can be measured through the two columns θ_{e-1} and θ_e in the sinogram, for the sinogram exactly reflects the shift. To find v, we used a certain section of e-th column and the section will be compared to the part of $(e-1)$-th column. Here, calculating v is an issue of the optimization problem and $f_e(t)$ has an absolute minimum at $t=v$ and $n=e$.

$$f_n(t) = \frac{1}{m}\left\{\sum_{k=1}^{m} |p_{n-1}(k+s-1) - p_n(k+s-1+t)|\right\}, -s < t < s$$

A total pixel number m is used in calculation. s is the starting point in the $(e-1)$-th column. $p_i(j)$ indicates the value of a pixel position at i-th column and j-th row in sinogram; $p_i(1)$ indicates the initial pixel point. If the object's shadow length in the sinogram is small enough compared to the projection size, $m=(1/2)*ny$, $s=ny/4$ is enough to use (ny is the total vertical pixel number). t is an integer and indicates translation. To simplify the calculation, we assumed that the pixel length is the unit length. To obtain the real value of v, it is possible to use the symmetric axis of a quadratic equation with $v-1$, v, $v+1$ and their f_n.

For example, the values of v=49, and θ_e=90° were obtained when the sinogram of Fig. 3b was analyzed. Any abnormal peaks were checked to figure out θ_e in the graph where x-axis indicates the angle and y-axis indicates the average difference value v, which is the distance between two columns of t=0.

After finding θ_e, we calculated r by the minimum value of t, $0 \leq t \leq 60$. Using the vertical movement value driven from the following formula,,the sinogram of Fig. 3b was transformed to an ideal one shown in Fig. 2a. Generally, it will be transformed to an similar-to-ideal one which satisfies the optimization formula $Vn=49*\cos(\theta_n-90^\circ)(\theta_e \geq 90^\circ)$, because we don't exactly know the column information of the ideal sinogram at θ_e.

Figs. 4a-4c show how we can apply the orthogonal translation algorithm to the real projections.

Figs. 4a-4c are sinograms and reconstruction images of a layer of Hanford soil in a polyether ether ketone (PEEK) column from National Synchrotron Light Source (NSLS) X2B beamline at Brookhaven National Laboratory (BNL). The third pictures in 4a-4c are the magnified images of the white frame of the reconstruction images in the middle.

Through the analysis of the sinogram of Fig. 4a, the specific $f_e(t)$ value was found at the discontinued spot; it was expected that a vertical translation error arose between the 360th and the 361th projections. For the middle panel, we used the RA of part B to minimize the error coming from two distinct RAs.

We applied our formula V_n to the sinogram of Fig. 4b, which brought us a sinogram with the continuity and a better reconstruction image. The area with high x-ray impermeability is moving along inside the sinogram showing a sinusoidal pattern (black arrows). In its reconstructed image, this area is placed in the upper right part (white arrow).

In Fig. 4c, the center of the x-ray impermeable material is set as the fixed point and it is applied to the function $T_{0,\phi}$ representing the virtual rotational axis of the sinogram; the point is now the line across the center in the sinogram (black arrows). It is placed on the center of the image in the reconstruction (white arrow). It is also noticeable that its reconstruction image is much clearer.

If only we know the angle θ at the moment of parallel translation error, we can figure out the distance of error using a similar technique we used for vertical translation error compensation; the parallel translation

error is corrected in the same way. The formula for this is presented below. (See Fig. 3a)

$$P_n=p*sin(\Theta_n-\Theta_e), n \geq e \text{ (or } n<e)$$

P_n is the distance to which the n-th column has to be moved in the sinogram.

Correction Algorithm

In the real settings of computed tomography (CT) system, the translational error is not only either a horizontal or vertical error but also a combination of both. Thus, a solution for the orthogonal translational error is not general enough. As we mentioned earlier, the horizontal shift of an object is hard to detect on the projection image and thereby, hard to calculate. This leads us to a need to approach this issue using a fairly new concept and a point of view. Knowing that the errors in the real settings are complicated and often a mixture of different kinds, one should start with understanding and defining the relationship between the real space and the sinogram, which is actually a projected and reconstructed version of real space, so as to further use it to draw a general and automated method of correction.

Ideally, the centerline of a sinogram is made up of the projection of RA. Any single point in the real space will move on a circular trajectory rotating around the RA and this will correspond to a function on the sinogram. Let's say there is a point p and it moves on a circular trajectory, this point p will be transformed into a curve on the sinogram and represented by the sinusoidal function $T_{r,\phi}$.

The circular trajectory of a point p in the real space corresponds to a curve drawn by the sinusoidal function in the sinogram. (2)

$$T_{r,\phi}(\Theta)=r*cos(\Theta-\phi), 0 \leq \Theta<180^\circ$$

We defined r is the distance between the rotation axis and the point p. Θ is the projecting angle, and ϕ is the angle between the line $\overrightarrow{Op}$ and the orthogonal line to the projection angle at $\Theta=0$(Fig. 4). O is the RA. In ideal cases, the center O is converted to $T_{0,\phi}$ in the sinogram, but not in the actual sinogram.

Fig. 5 shows the sinogram and its reconstruction image with which we figured $\overrightarrow{P_{CA}}$ of each column in Fig. 3b sinogram and align them on the function $T_{50,30^\circ}$.

Using (1) and (2) which were mentioned earlier in this disclosure, we can alter an inaccurate sinogram to a correct one. $T_{r,\phi}$is a function that shows how a specific point p in the real space moves on the sinogram. It means that we can keep tracing a point of the real space on the sinogram and further use it as we intend to. In other words, if a point p in the solid specimen rotates on the stage and the projected curve drawn by the movement of p for each angle is the same as the sinusoidal curve by $T_{r,\phi}$ in the sinogram, then the projected trajectories of other points in the specimen should satisfy the projected curves by $T_{r_n\Phi_n}$ and all points in space satisfy the consistency condition. Being the center of a circle, the point p on the sinogram in Fig. 5 will be always on the center of the projection shadows. It follows the curve marked as a solid line on the sinogram since the specimen itself is off the center (see the sinogram of Fig. 5). The point p is a center-of-mass for a circular object if the object has an identical medium and acts as a fixed point to represent the same spot even when the projection angle changes. With the point p translated on the function $T_{0,\phi}$, that is to say, with each column in the sinogram moved so that the point p is on the center and the solid lined curve is now laid linearly on the center line of the sinogram, the center of an object will match exactly to the center of projection and the sinogram will become linear. When applied to a real space, this virtual translation has the same effect as we physically set the center of an object on the RA.

Accordingly, as shown in Fig. 1, we determine at least one fixed point of the object in step S2 and let the fixed point to be the virtual rotation axis such that the fixed point to be a straight line across the center of the sinogram(step S3).

Then, relative positions of the points other th an the fixed point of the object relative to the fixed point in the sinogram are calculated in step S4.

Based on this calculation of the relative positions of the points, this sinogram may be transformed into a reconstructed image through the inverse Radon transform(step S5).

Nevertheless, real objects are not always cylindrical. They rather come in much more complicated structures, and as a result, it is not an easy issue to define a fixed point on the projections. We came up with a new physical concept called the center of attenuation (CA) to make this issue simpler. The CA is a similar idea with the center-of-mass, but is different in a way that a unit particle of an object is expressed not by the X-ray density but by the x-ray mass attenuation coefficient (MAC) which is measured by the initial energy. We can use any other X-ray coefficient. In general, the center of mass estimated by X-ray densities in projection images cannot play a role in our FP because of the followings: the X-ray absorption for the thickness of specimen is not linear and the specimen size is lager than the charged coupled device (CCD). Our assumption for using MAC is that there is co-relationship between a unit voxel of real object and a unit voxel of reconstruction i mage. For 3D, the CA calculation requires the object part in a subset of common layers. We define a common layer that a plane envelops the same whole part of the object' s axial level in the real space and perpendicular to the RA.

When the relationship between the change of x-ray intensity on a logarithmic scale and the specimen length is not linear after the x-ray beam penetrates the specimen, it should be first transformed into something with linearity and utilized to figure out the CA. (3)

The value of MAC should be changed into the one expressed in length to calculate the CA, we call the modified density (MD) relating to the sum of mass attenuation coefficient in a projection set.

When an x-ray beam is shot to an object, the object absorbs certain amount of the energy and the rest of attenuated energy arrives on the detect or. Then we get the projection image. As any object has a center-of-mass of classical mechanics, we assumed that any object has an invariable center of MAC, and it is fixed on a certain spot, either inside or outside of the

specimen, acting as a fixed point that does not change depending on the projection angle. This fixed point can be calculated from the projection images obtained from each angle of x-ray penetration. It will lie on the sinogram satisfying the $T_{r,\phi}$ function that was mentioned earlier and this is how we get an ideal sinogram pattern.

Correction of translational error in 2D using CA

The calculation for CA is very similar with the one for center-of-mass of classical mechanics. First, a virtual rectangular coordinate and unit cubes are adopted in the real space and each vertex is the whole number on the coordinate. Let's assume that the specimen placed in the coordinate is composed of n unit cubes. The i-th cube among the n cubes of the object has mass attenuation coefficient μ/ρ (MAC) for the given unit cube related to voxel length on its designated location and it is represented as a_i which can be linearly calculated through a series of calculation processes. (We can use other coefficients related to X-ray transmittance.)

Below is the formulation we used to mathematically identify the location of CA and on the coordinate.

$$\overrightarrow{CA} = \frac{1}{A}\sum_{i=1}^{n} a_i \vec{r_i} \qquad (2)$$

a_i is $c \times \frac{\mu_i}{\rho_i}$, and c satisfy that an unit voxel density for the given initial energy has the same value of a_i. A is the total sum of a_i and a constant value. A is defined in a subset of a whole common layer set (this will be discussed in 3D) and n is the total grid number of the object in a subset of common layers of the real space. $\vec{r_i}$ indicates the center of i-th grid. $\overrightarrow{CA}$ is one of the fixed points in real space and particularly significant in that it will be always projected and we can trace it later on the projections. So, $\overrightarrow{P_{CA}}$, a projected position of $\overrightarrow{CA}$ can be calculated in the projection image as below

$$\overrightarrow{P_{CA}} = \frac{1}{A}\sum_{i,j} p_{ij} \vec{r_{ij}}$$

Here we see that $A = \sum p_{ij} = \sum_{i=1}^{n} a_i p_{ij}$ is the (i, j) pixel value of the projected specimen in the 2-dimensional projection and $\overrightarrow{r_{ij}}$ is the center of the pixel. As the a_i is calculated by MAC, the p_{ij} also should be linearly expressed and modified by the sum of the related a_i.

In the projection image, the attenuation value of the area except for the computational domain for the object shadow should be zero in the ideal status. If it is not zero, $\overrightarrow{P_{CA}}$ might not be able to act as the fixed point. So we need to modify the attenuation value of this area to have at least the average of zero when it is not exactly zero, ensuring the same amount of MD is added or subtracted to the p_{ij} area.

$\overrightarrow{CA}$ in the real space becomes a specific point that we know and it is projected to be $\overrightarrow{P_{CA}}$ and expressed as the $T_{r,\phi}$ function on the sinogram. The center of projection is always the center line of the sinogram. Therefore, when $\overrightarrow{P_{CA}}$ from each angle of x-ray beam is translated onto the center line $T_{0,\phi}$ of the sinogram, it can be considered the same as the fixed point of an object is placed on the RA. In other words, we are able to get rid of all the translation errors in the 2-dimensional space by translating $\overrightarrow{P_{CA}}$ of each projection on the $T_{r,\phi}$ function. Since $\overrightarrow{P_{CA}}$ of each projection is one of the projected fixed points, all fixed points can be translated on $T_{r,\phi}$ and expressed in the sinogram. For real samples, the center line of the sinogram does not represent a RA. In this case, we define that the center line is the virtual rotation axis representing $T_{0,\phi}$, and rearrange any fixed point on $T_{r,\phi}$ to make one of ideal sinograms.

Figs. 6a-6c show how we applied this idea to the real images which illustrates analysis of a partial image of human lower jaw including the teeth. Fig. 6a shows an image of the sample and its sinogram (The object is on the lower right side of the stage). The $\overrightarrow{P_{CA}}$s of all projections are marked black in the sinogram. They follow the circular trajectory in the real space, therefore show sinusoidal graph in the sinogram. Fig. 6b shows a sinogram with artificial translation errors added to the sinogram of Fig. 6a including vertical and horizontal movement at each angle and its reconstruction image.

The $\overrightarrow{P_{CA}}$s, the black marks are all scattered. Fig. 6c shows a sinogram that we aligned $\overrightarrow{P_{CA}}$ of the sinogram of Fig. 6b on $T_{0,\phi}$ and its reconstruction image. The $\overrightarrow{P_{CA}}$s are arranged linearly on the center of the sinogram. $\overrightarrow{CA}$ is on the center of the stage and the image is ideally restored.

Analysis of 3D Image Reconstruction from a Projection Image Set

There are only translation errors in the two dimensional projections. However, other kinds of error have to be taken into consideration when it comes to three dimensions. Mainly, three kinds of errors can be discussed; a translation error caused by the shift of a specimen, a tilting error caused when the RA is tilted, and the rotation error that is caused when a specimen spins on its own axis.

A translation error is the error that happens when the object is moved by any chance during the beam time, and the movement can be in three directions in the 3D space. A compensation for this error can be done through just the way we did with the translation error in 2D space, bringing $\overrightarrow{P_{CA}}$s on the $T_{r,\phi,h}$ function.

$T_{r,\phi,h} = (r*\cos(\theta-\phi),h), 0 \leq \theta < 180^\circ$, where h is a level of a common layer of a projection set.

The translation error in 3D is different from the one in 2D in that we should adjust the layer of FPs so that the FP is on the same layers. For specific projection sets whose density preserve linearity, we first set a specific layer of projections as height h, and translate $\overrightarrow{P_{CA}}$s onto the $T_{r,\phi,h}$ function of this layer. This is a significant procedure in the 3-dimensional reconstruction because it is simply not possible to reconstruct an image well using projections of different layers. To make our calculation easier, we will place the CAs on the RA (r=0) of the projections' center layer (h=0) and this process will be more beneficial if one considers using an optimization method to correct tilting errors. By doing this, we can compensate most of the translation errors and the CA is on the center of projection (Figs. 7a-7d).

Figs. 7a-7d show an object of prolate spheroid is located on the rotating stage, which has the center of CCD as the RA, and rotates for the

360 degrees. The CA is at the height of h=0, and the distance from the center is r=d. The azimuthal angle of the object is 0 degree when the θ is zero. The white dot and the line represent where $\overrightarrow{P_{CA}}$ lies against each θ. Fig. 7a shows the sinogram of the h=0 layer when the object is at θ=90° and there is not any known err or. Fig. 7b shows the sinogram of the h=0 layer when there was a translation error at θ= 90° . The location of the object in the involved layer is moved to the lower right on the stage and its shape is narrower, compared to that of Fig. 7a. This is reflected in the sinogram; the location of shadow and its width have changed (Look at the magnified part of the sinogram). In Fig. 7c, the $\overrightarrow{P_{CA}}$ in the projection of Fig. 7b was translated vertically to the stage, exactly on the layer in which the $\overrightarrow{P_{CA}}$ without error exists, h=0. The location of shadow has not changed, however, the width now becomes identical with the other θs in the sinogram. When we aligned $\overrightarrow{P_{CA}}$ on the function $T_{0,\phi,0}$, the $\overrightarrow{P_{CA}}$s were all gathered onto one dot on the center of the stage, and the sinogram became linear as in Fig. 7d. For the other case, we should consider layers where the error occurs. Our numerical results illustrate how the translation error can be compensated using common layers which include fixed points (Fig. 13). Fig. 13a shows the sinogram with translation errors θ_e=60° at the blue colored axial level of the CCD (right pan el) and two projection images at θ=45° and, θ=90° (left and middle panel, respectively). In order to fix the error, we first set two cleared fixed points in the projection sets at bo th angles (red and orange colored circle are the first and second fixed points, respectively). However, those fixed points are placed on different axial level of the CCD. For this case, we adjust the projection images via the high density areas by rearranging the projection set where each high density area is located on the same axial level, called the common layer (Fig. 13b). Once this process is completed, the high density area appears its trajectory in the sinogram over θ less than $60°$. The shape of the high density area can be considered as a circular shape and the center of the circle can be a projected fixed point. To fix the translation errors, we translate the projected fixed points onto the $T_{r,\phi,h}$ function of the common layer. To make our calculation easier, we

place the projected fixed points on the $T_{0,\phi,h}$ and then the projected fixed points are located on the projected RA. Adjusting common layers is a significant procedure in the 3-dimensional reconstruction because it is simply not possible to reconstruct an image well using projections of different layers.

Analysis of tilting Error in 3D

In 3-dimensional space, it is important to consider tilting errors because a tilted image carries information from different layers and consequently induces a flawed image reconstruction. Thus, if we compensate the tilting error, it means that we make one layer to carry all the information about a single part of an object. To categorize and analyze tilting errors, we should further discuss about the object itself and the stage that it is placed on. We will not call the case of tilted object an error. It is because we can make a reconstruction image without any correction procedures in this case. When it is the RA that is tilted, one should make sure that the tilting error is corrected.

If a cylindrical object on the stage is tilted and projected, we cannot tell whether it is the object or the RA of the stage that is tilted, only by looking at the projection image. However, those two should be distinguished and defined. When the RA is upright and only the object is tilted, it should not be called a tilting error and consequently, the projection set should not be corrected. Instead, it should be considered as we put some other object which originally has a tilted shape. As it sounds ironical, one would hardly get an ideal projection set if this kind of error is corrected because the original projection set was already correct. Nevertheless, it is hard to tell the difference between the tilt of an object and the one of a RA in the projection image; one should turn to the sinogram in this case because these errors will be seen more easily and clearly in the sinogram.

We can make sense of this logic better with the following Figs. 8a-8c. The Fig. 8a shows when the object is tilted whereas Fig. 8b shows when the RA is tilted. The sliced image of the specimen upon a same layer is identical in those cases. However, their sinograms show definitely different patterns.

In case of a tilted object, the sinograms of its top and bottom follow sinusoidal functions. When the RA is tilted, however, the heights are the same with the ones in the former case, while the patterns of the top and bottom go linear starting from each height. The sinograms obtained from Fig. 8a are the ideal sinograms which will produce a correct reconstructed image; the others will not give us a correct reconstructed image since the layers are all mixed up during the projection. In short, we will not call the case of tilted object an error. It is because we can reconstruct a correct image without any correction procedures in this case. When it is the RA that is tilted, one should make sure that the tilting error is corrected.

In terms of the tilted RA, we can further classify two cases of leaning in detail; one is of a vertical direction and the other is of a horizontal direction toward the x-ray beam. The former is shown in Fig. 8b and the latter is shown in Fig. 8c. In a vertical tilt, the polar angle increases when the azimuthal angle is either 90 or 270 degrees. On the other hands, the polar angle increases when an azimuthal angle is either 0 or 180 degrees in a parallel tilt. The azimuthal angle increases counter clockwise against the beam. The ideal RA which stands upright without any tilting error is assumed to be the reference for the polar angle.

It is the case of a vertical tilt when the RA is tilted against the axis of whole projection and the stage is rotating with the tilted RA. If we assume that the common layer is also tilted in parallel with the stage, namely tilted by the same angle in the projection, the projection information is now about a single layer, not mixed with the ones about other layers. Hence, if we only know how much the RA is tilted, and carry out a rotation compensation on the whole projection rotating around CA, we can find the common layer that we can concentrate on. Contrarily, the parallel tilt carries information about more than just one common layer and it is hard to get an ideal sinogram pattern in this case.

It is the projection image of a cylinder standing perpendicularly on the RA of the stage in Fig. 9a. When translated without tilts, the shadows are of same shapes even when the locations on the projection are different.

Fig. 9b shows a projection image of the cylinder that is leaned in parallel with the beam and its depth of the shadow is changed, meaning the information of the image is changed. The shadow is darker than before; the information of the image is changed and the restoration with the projection is not easy in this case. One can see the projection image of the same cylinder tilted vertically in Fig. 9c. It is shown that the depth of shadow remains unchanged, even though the object is tilted; the projection information is not changed. In this case, it is possible to restore with the projection image.

Correction algorithm for the vertical tilting of an object

In correction process, the priority is to know by which angle the RA is tilted. The whole projected images will be corrected accordingly to the tilted angle using the center line of whole projection , $T_{0,\phi,h}$, as a fiducial line. To figure out the specific angle that the RA is tilted by, we used our CA in this study. Assuming that we virtually collected the every $\overrightarrow{P_{CA}}$ of each projection we get from a specimen and placed them on the charged coupled device (CCD), we thought that they would form a virtual line segment just like in Fig. 8b. In fact, the line segment of $\overrightarrow{P_{CA}}$ stands for the trajectory of CA, and the RA is perpendicular to it. If this RA and the vertical line makes a certain angle, it is the angle by which we will rotate the projection set to meet the ideal one which doesn' t have the tilt error.

In this disclosure, we categorized the errors that possibly take place during the beam time. We can modify most of the errors using FP and enable to improve the reconstruction image. We call new reconstruction image as the ideal reconstruction image from now, which is coming from ideal sinogram pattern. There are two cases for the tilting errors. When it is the vertical tilt, we get the ideal reconstructed image. In case of the parallel tilt the information of different layers are mixed up. Mostly, the tilting error is a mixture of both vertical and parallel tilts; the optimized projection set in which the vertical error is modified is the best deal in this case.

The method to figure out the angle of the vertical tilt is already discussed earlier. Even in a parallel tilt, the tilted angle can be sought

with the same method.

The angle of parallel tilt, α, satisfies $\sin\alpha = \frac{b}{a}$. Here, a means the major axis and b does the minor against the trajectory of CA. Whether the orientation of trajectory in the projection is clockwise or counter clockwise depends on whether the azimuthal angle of RA is 0 degree or 180 degrees. This method can be also applied to the mixed error of vertical and parallel tilts.

Fig. 10 shows a trajectory of a fixed point when there were several errors during beam time.

When the translation error and tilting error occurred partially, we can get the RA of each piecewise continuous section by analyzing the trajectory of fixed point in each section. We can obtain the well reconstructed image when we modify the projections using these RAs.

The CA we suggested in this disclosure will function as the fixed point that is one of the intrinsic factors of an object. It works as an invariable point inside (sometimes outside) of an object which does not change even when the object is moved, or the RA is tilted. Nonetheless, we have to calculate this CA from the projected image so as to utilize it, which results in one limitation that the intensity variation of the beam reaching each cell of the CCD in the formula for $\overrightarrow{P_{CA}}$ should be linearly proportionate to the length of the specimen. That is, the attenuation value of each cell which consists of the image from the projection should have some linear relationship with the length of the specimen or at least should be changeable to have linear relationship.

As other studies have pointed out, most of the objects maintain the linear relationship in the soft x-ray area. We should be able to modify them if it is the object that does not present linear relationship or it is in other x-ray area than soft x-ray. If the material that consists of the specimen is relatively identical and the x-ray attenuation function against length is a one-to-one function having the single attenuation coefficient (AC), the linearity can be granted with a simple modification. If the AC is composed of materials that are not identical, what we can do is to ensure the linearity to the projected image of an object that has the shortest section

of linearity guaranteed.

To obtain well reconstructed image, we should make sure to get a consistent x-ray density against the object regardless of projecting angles. In reality though, we sometimes get the different x-ray density according to the projecting angle changes, and then, the value of A also should be changed in the formula applying the CA. It would be difficult to generally use CA for the reconstruction if the location of CA depends on the changes of x-ray density and the A value. The changes of x-ray density (according to the angle) will appear in the sinogram in forms of the shadow intensity. Nonetheless, it won't affect the pattern of the sinogram.

Figs. 11a-11b show the cases when the x-ray density of projection is changed during the beam time. Fig. 10a shows the case where the sinogram and its reconstruction image when the x-ray density of projection in Fig. 6a is decreased by half after θ=90° , and Fig. 11b shows the sinogram and its reconstruction image when the CA was applied to the projection with changed x-ray density.

In Fig. 11a, the pattern of ideal sinogram was maintained although there was a 50% decrease in x-ray density from the 90 degrees of θ. The reconstructed image using the sinogram with the CA and the $T_{r,\phi,h}$ function applied (Fig. 11b) showed no difference in terms of image itself when compared with the reconstructed image of Fig. 11a, and the image of specimen in Fig. 11b was laid in the center. This proves to us that the location of CA does not vary despite the changes of A value against each θ drawn by the different x-ray density. Also, we may be able to get a better image if we mathematically modify the x-ray density in order to even up the A value. Furthermore, if we can find the minimum value of A preserving the linearity, we can obtain sufficiently large value of A by mathematical modification. For the total amount of radiation dose, we can get the better reconstruction images by increasing the total number of projection images with low dose X-ray.

The CA in our study is expected to significantly contribute to a better image reconstruction in x-ray tomography and to be utilized as a versatile

tool. When the specimen is mixed up with materials having greatly diverse ACs to the extent where it is out of linearity, it is hard to compensate the unlinear area and this may result in errors. And it is not beneficial to use the CA in those cases when the specimen is projected with impermeable materials like metal to make it distinguished. It is better to project the specimen itself without any other distinguishing material when anyone wants to use CA in image reconstruction. The ring artifact due to the CCD defect could be another hurdle in CA application. We need to correct the ring artifact beforehand; the correction itself can also raise some changes in reconstruction errors.

In our study, we realized that every single point on the stage shows a periodic motion around the RA and the motion will be reflected as a sinusoidal function on the sinogram. If we try to optimize the errors, the optimization was only done to the moment of the error occurred in the sinogram, and the sinogram was vertically moved to connect the discontinuity without talking the sinusoidal function into account. This, unfortunately, leads to flawed image reconstruction. So, we had to use a formula like V_n to modify our sinogram. This is shown quite intuitively in Figs. 12a-12c which show optimized reconstruction images with various optimization methods. An object was placed on the exact center-of-rotation, and the ideal sinogram of the object is found in the Fig. 12a. If there is a vertical error at the 90 degrees, the sinogram will be like Fig. 12b, and the error will be also seen in the reconstructed image. Simply moving vertically and linking the sinogram will bring us a sinogram like Fig. 12c and it will still yield incorrect, but different kind of reconstructed image. Our formula D_n, when the sinogram after the error is corrected, will bring a correct reconstructed image that is the same with the original image. Yet, it is not considered as a perfect reconstruction because what we used is the information of θ_{e-1}, not the exact point of error, θ_e, in optimization with the formula D_n. Therefore, we eventually need the function $T_{r,\phi,h}$, using CA or FP.

In spite of the benefits of categorization, the errors often come about not as we categorized, but as a mixture of different kinds. The application

will be much more extended if we can discover more than one fixed point besides CA and we can utilize each of them to the $T_{r,\phi,h}$ function. We showed the example of this idea in Figs. 4a-4c. If there is an area whose boundary is definite and x-ray impermeability is comparatively high, it will be distinguished in the most of projections. We might be able to use its center as another fixed point. We searched for the trajectory of the fixed point in the sinogram of Fig. 4b, and applied it to the function $T_{r,\phi,h}$. It was transformed into the function $T_{0,\phi,h}$ in Fig. 4c.

Here, we see that it provided us with a clearer image when the $T_{0,\phi,h}$ function was applied to the fixed point. It is expected most of the errors will be corrected when the fixed point and the CA applied in the $T_{r,\phi,h}$ function in case of mixed errors.

Other variations to the disclosed embodiments can be understood and effected by those skilled in the art in practicing the claimed invention, from the study of the drawings, the disclosure, and the appended claims. In the claims the word "comprising" does not exclude other elements or steps and the indefinite article "a" or "an" does not exclude a plurality. A single processor or other unit may fulfil the functions of several items or steps recited in the claims. The mere fact that certain measures are recited in mutually different dependent claims does not indicate that a combination of these measures cannot be used to advantage. A computer program may be stored/distributed on a suitable medium such as an optical storage medium or a solid-state medium supplied together with or as part of other hardware, but may also be distributed in other forms, such as via the Internet or other wired or wireless telecommunication systems.

CLAIMS

1. A method of reconstructing an image in a computed tomography, the method comprising:

obtaining a sinogram of an object;

determining at least one fixed point of the object;

letting the fixed point to be a virtual rotation axis such that the fixed point corresponds to a straight line across a center of the sinogram;

calculating relative positions of points other than the fixed point of the object relative to the fixed point in the sinogram; and

reconstructing an image based on a calculation of the relative positions of the points.

2. The method according to claim 1, wherein the sinogram is obtained from a set of projection shadows, and

wherein obtaining the sinogram of the object comprises approximating the set of projection shadows by a linear interpolation.

3. The method according to claim 1, wherein calculating relative positions of the points is performed using a sinusoidal function $T_{r,\phi}$

$T_{r,\phi}(\theta)=r*cos(\theta-\phi)$, $0\leq\theta<180^{\circ}$, and

wherein r is a distance between the rotation axis and a point p, θ is a projection angle, ϕ is an angle between a line $\overrightarrow{Op}$ and an orthogonal line to the projection angle at $\theta=0$, and O is the rotation axis, provided that the fixed point is translated on the $T_{0,\phi}$.

4. The method according to claim 1, wherein the fixed point is a center of attenuation $\overrightarrow{CA}$ represented in a vector form as $\overrightarrow{CA}=\frac{1}{A}\sum_{i=1}^{n}a_i\vec{r}_i$,

wherein a_i is $c\times\frac{\mu_i}{\rho_i}$ and c satisfy that an unit voxel density for a given initial energy has the same value of a_i, wherein A is a total sum of a_i

and a constant value, wherein A is defined in a subset of a whole common layer set and n is a total grid number of the object in a subset of common layers of the real space, $\vec{r_i}$ indicates the center of i-th grid,

wherein the projected position of $\overrightarrow{CA}$ is calculated as $\overrightarrow{P_{CA}}=\frac{1}{A}\sum_{i,j}p_{ij}\vec{r_{ij}}$, and wherein $A=\sum P_{ij}=\sum_{i=1}^{n}a_i$ and p_{ij} is a modified (i,j) pixel value of the projected specimen in a 2-dimensional projection and $\vec{r_{ij}}$ is a center of the pixel.

5. The method according to claim 4, wherein the center of attenuation is obtained using modified density into which is transformed to have linearity from an original density.

6. The method according to claim 4, wherein the center of attenuation is located either inside or outside of the object.

7. The method according to claim 1, wherein the fixed point is a specific geometric position of the object.

8. The method according to claim 1, wherein the fixed point is the center of an area whose boundary is definite and whose x-ray impermeability is higher than those in the other areas.

9. The method according to claim 1, wherein obtaining the sinogram of the object comprises obtaining a set of sinogram layers; and

wherein calculating relative positions of the points is performed using the sinusoidal function $T_{r,\phi,h}$

$T_{r,\phi,h}(\theta)=(r*\cos(\theta-\phi),h),\ 0\leq\theta<180^\circ$,

wherein r is a distance between the rotation axis and a point p, θ is a projection angle, ϕ is an angle between a line $\overrightarrow{Op}$ and an orthogonal line to the projection angle at $\theta=0$, O is the rotation axis, and h is a height of

a specific layer of projection

provided that the fixed point is translated on the $T_{0,\phi,h}$.

10. The method of claim 4, if a minimum value of preserving linearity can be found, sufficiently large value of A can be obtained by mathematical modification, wherein, for a total amount of radiation dose, reconstruction images will be better by increasing the total number of projection images with low dose X-ray.

11. The method of claim 1, wherein the fixed point is a point in space that can be discriminated or calculated by analysis of a projection image set.

12. A computer-implemented method for reconstructing an image in computed tomography, the computer including a processor, the method comprising:

obtaining, by the processor, a sinogram of an object;

determining or receiving, by the processor, at least one fixed point of the object;

translating, by the processor, the fixed point to be a virtual rotation axis such that the fixed point corresponds to a straight line across a center of the sinogram;

calculating, by the processor, relative positions of points other than the fixed point of the object relative to the fixed point in the sinogram; and

reconstructing, by the processor, an image based on a calculation of the relative positions of the points.

13. The method of claim 12, wherein the computer is embodied as a medical imaging device.

14. A non-transitory computer-readable medium having stored thereon

computer-executable instructions that when executed by a computer cause the computer to:

obtain a sinogram of an object;

determine or receive at least one fixed point of the object;

translate the fixed point to be a virtual rotation axis such that the fixed point corresponds to a straight line across a center of the sinogram;

calculate relative positions of points other than the fixed point of the object relative to the fixed point in the sinogram; and

reconstruct an image based on a calcuation of the relative positions of the points.

15. A system for reconstructing an image in computed tomography, the system comprising: a processor; an input coupled to the processor and configured to receive a parallel projection dataset; and a memory coupled to the processor, the memory including computer-executable instructions that when executed by the processor cause the processor to:

obtain a sinogram of an object;

determine or receive at least one fixed point of the object;

translate the fixed point to be a virtual rotation axis such that the fixed point corresponds to a straight line across a center of the sinogram;

calculate relative positions of points other than the fixed point of the object relative to the fixed point in the sinogram; and

reconstruct an image based on a calculation of the relative positions of the points.

FIG. 1

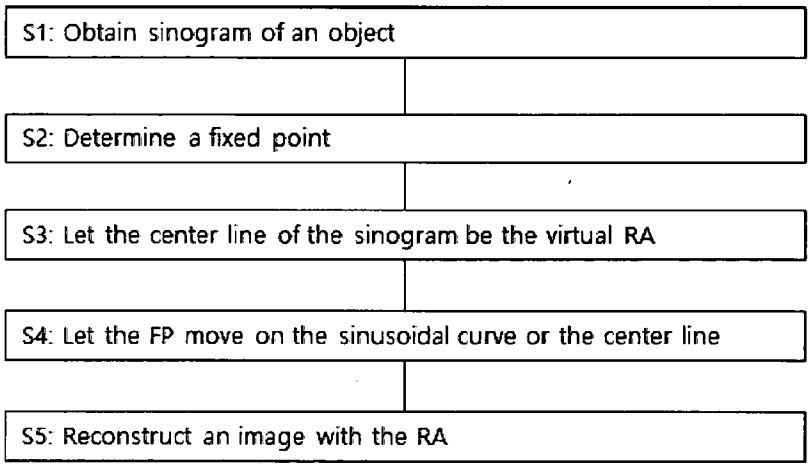
S1: Obtain sinogram of an object
S2: Determine a fixed point
S3: Let the center line of the sinogram be the virtual RA
S4: Let the FP move on the sinusoidal curve or the center line
S5: Reconstruct an image with the RA

FIG. 2a

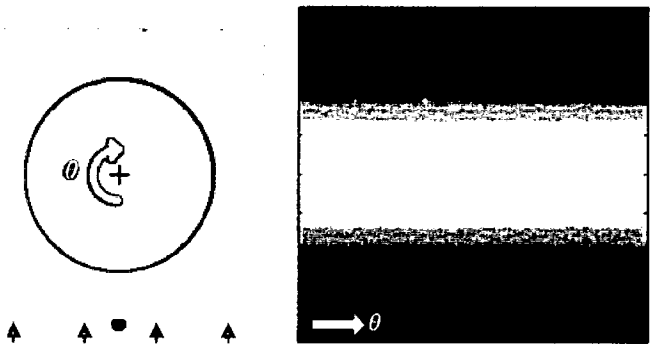
θ
θ

FIG. 2b

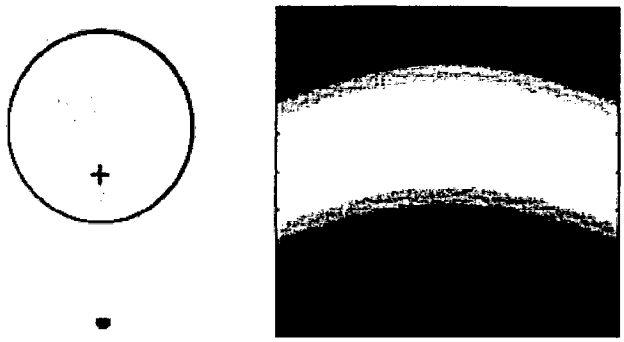

FIG. 2c

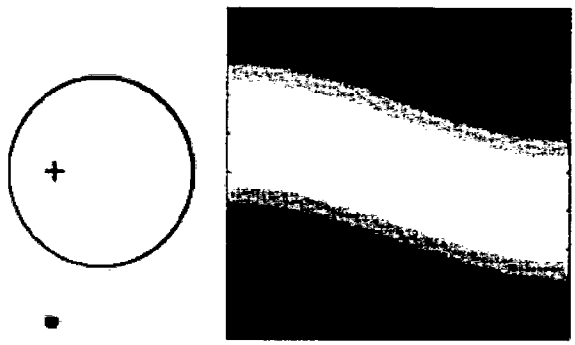

FiG. 3a

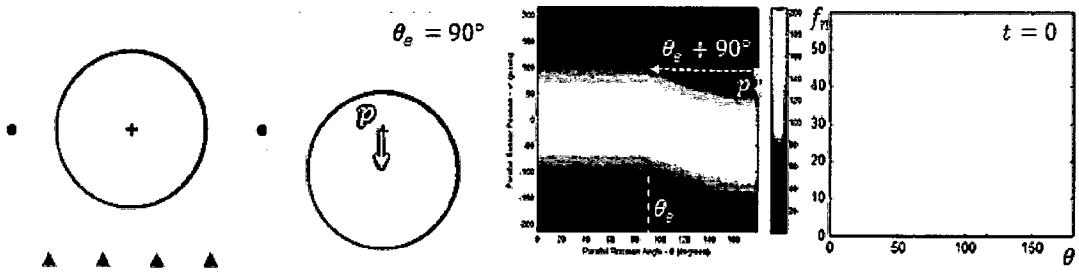

FIG. 3b

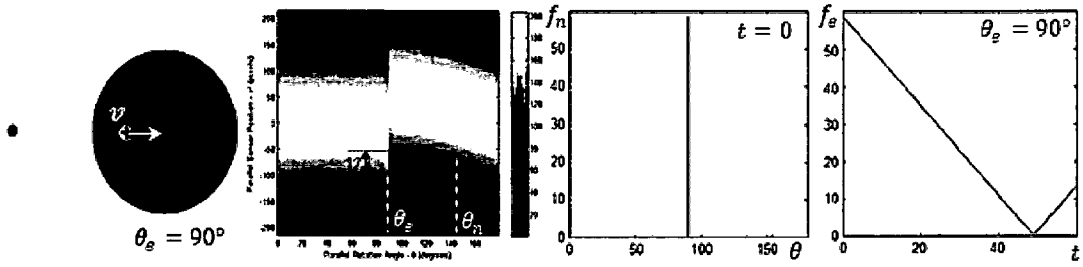

FIG. 4a

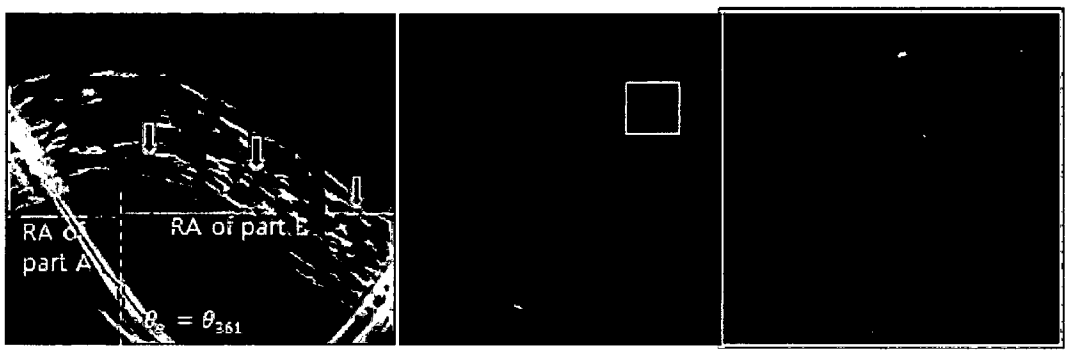

FIG. 4b

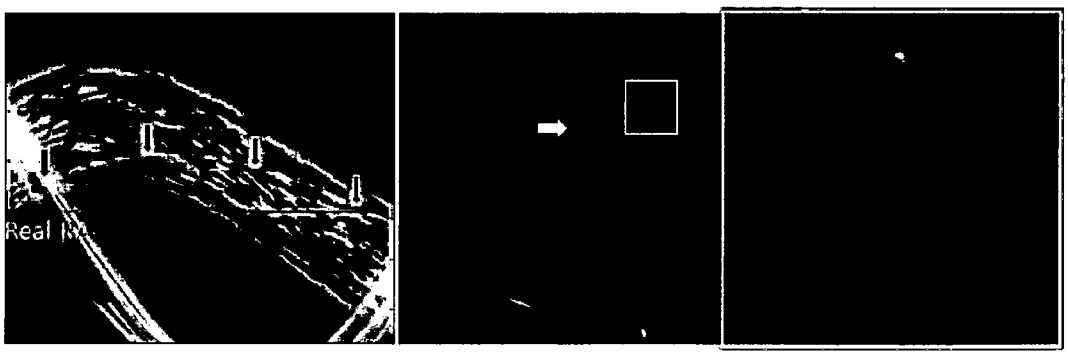

FIG. 4c

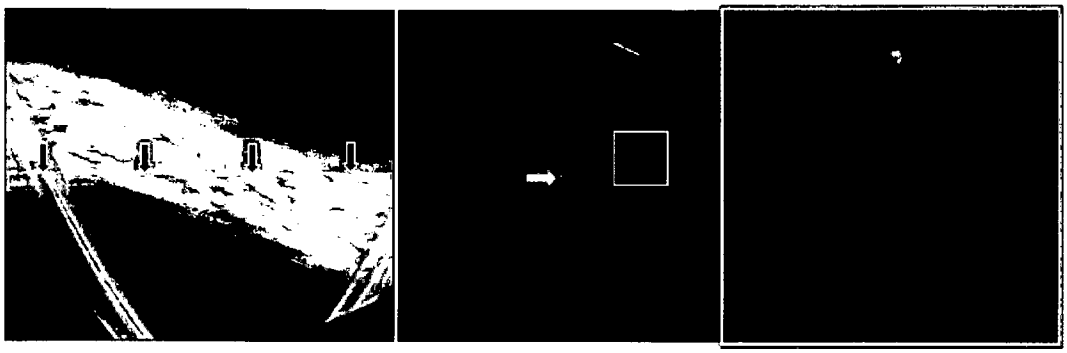

FIG. 5

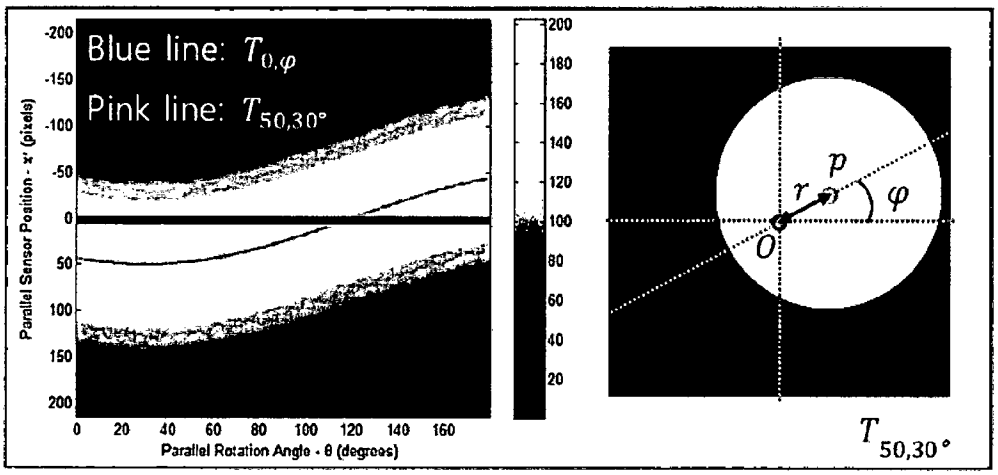
Blue line: $T_{0,\varphi}$
Pink line: $T_{50,30°}$
Parallel Sensor Position - x' (pixels)
Parallel Rotation Angle - θ (degrees)
p
r
φ
O
$T_{50,30°}$

FIG. 6a

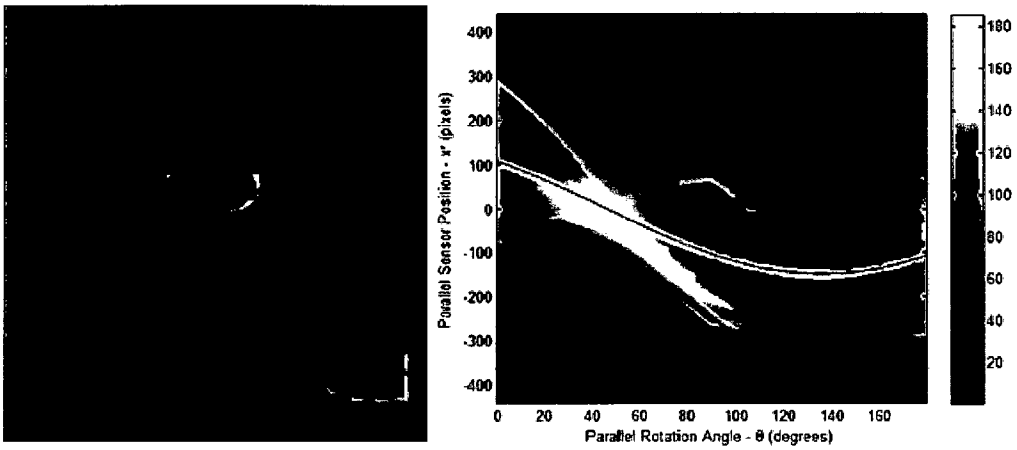
Parallel Sensor Position - r' (pixels)
400
300
200
100
0
-100
-200
-300
-400
0 20 40 60 80 100 120 140 160
Parallel Rotation Angle - θ (degrees)
180
160
140
120
100
80
60
40
20

FIG. 6b

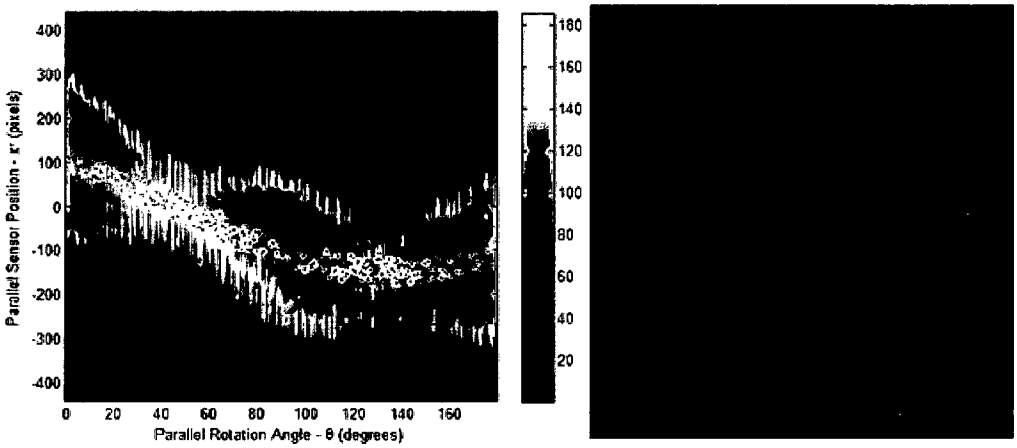
Parallel Sensor Position - r' (pixels)
400
300
200
100
0
-100
-200
-300
-400
0 20 40 60 80 100 120 140 160
Parallel Rotation Angle - θ (degrees)
180
160
140
120
100
80
60
40
20

FIG. 6c

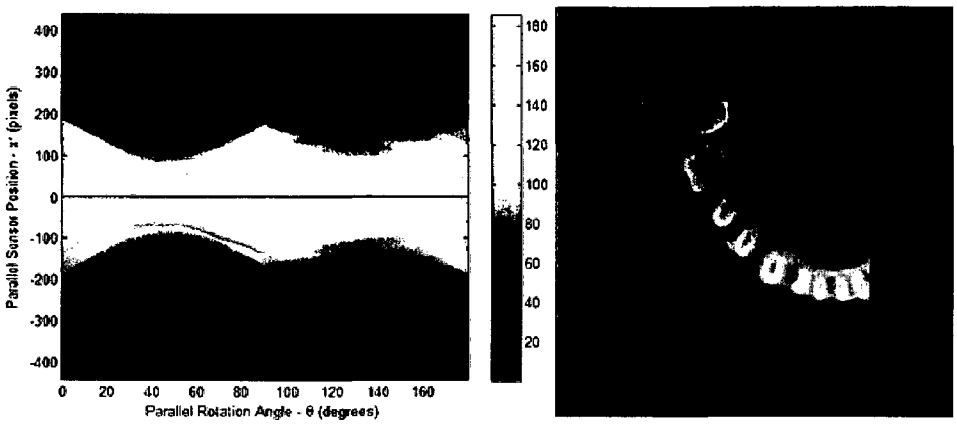
Parallel Sensor Position - x' (pixels)
400
300
200
100
0
-100
-200
-300
-400
0 20 40 60 80 100 120 140 160
Parallel Rotation Angle - θ (degrees)
180
160
140
120
100
80
60
40
20

FIG. 7a

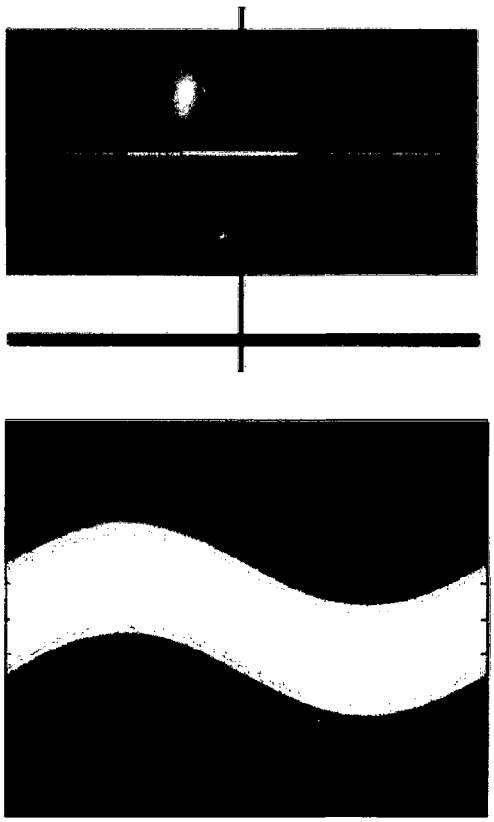

FIG. 7b

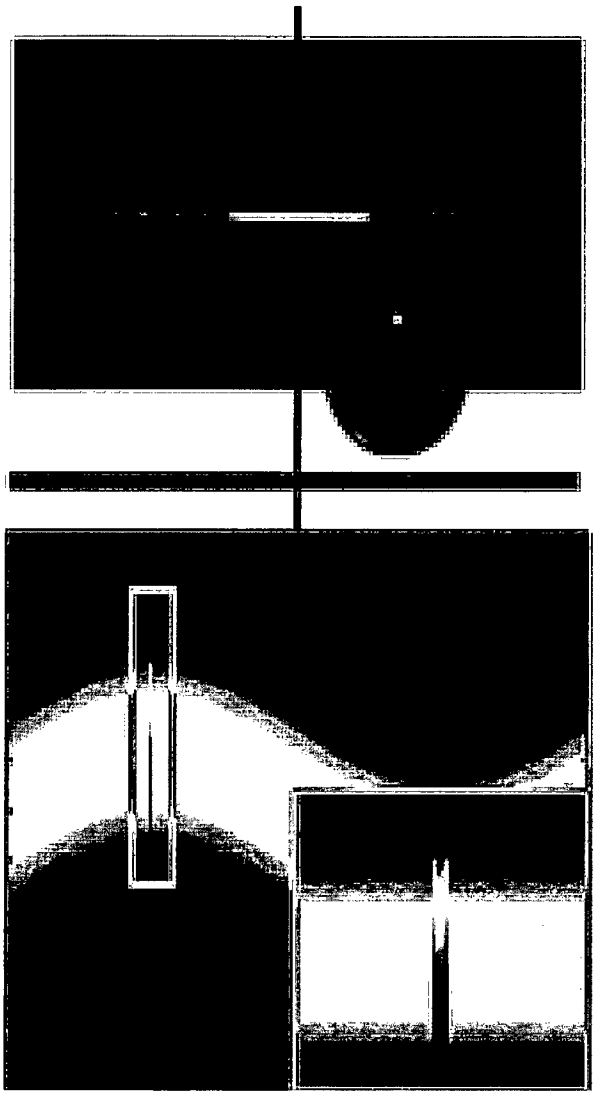

FIG. 7c

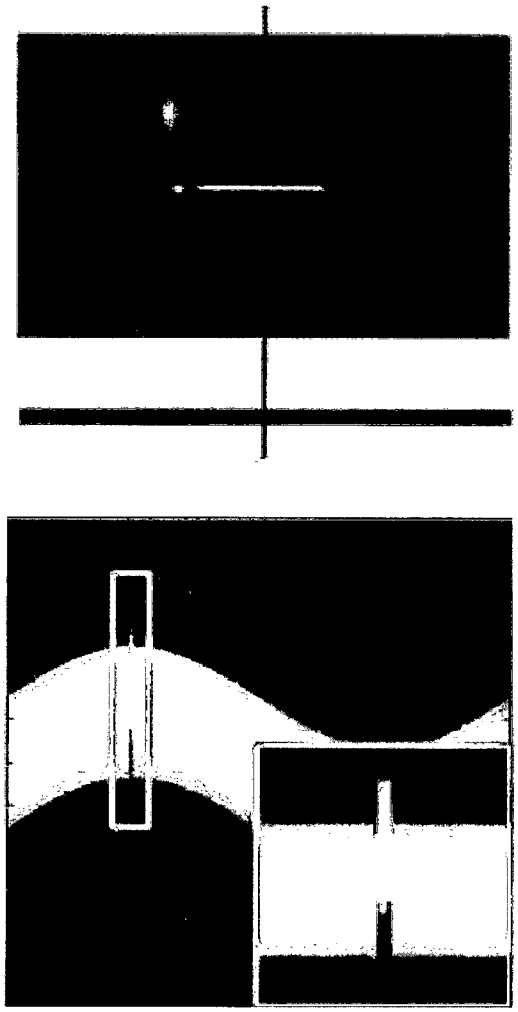

FIG. 7d

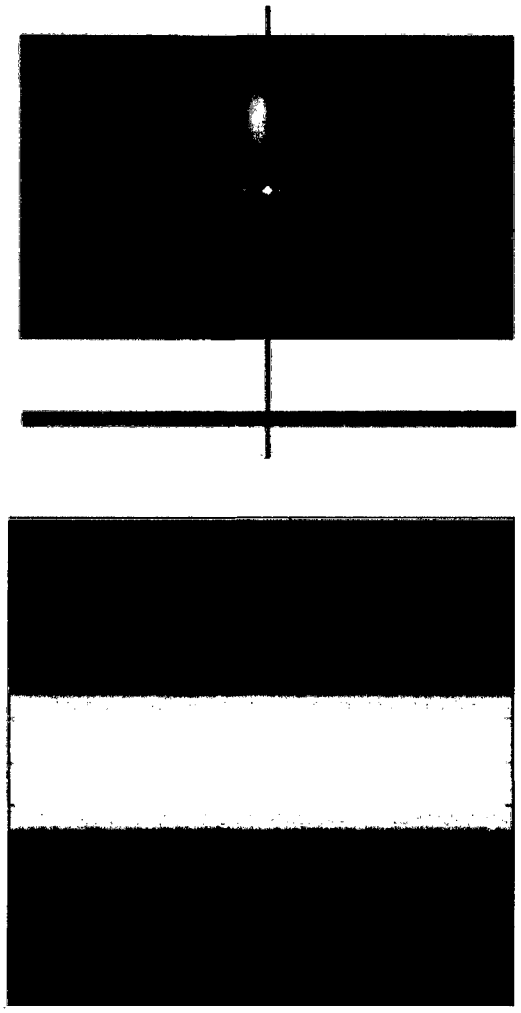

FIG. 8a

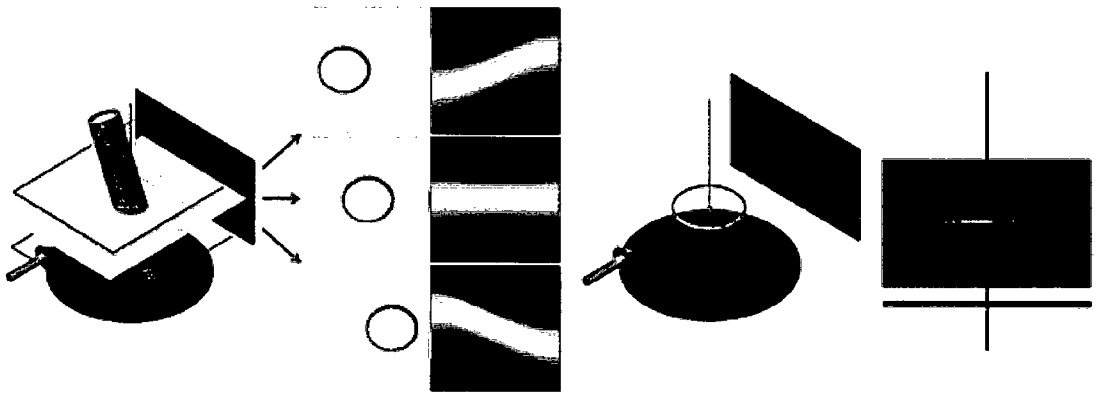

FIG. 8b

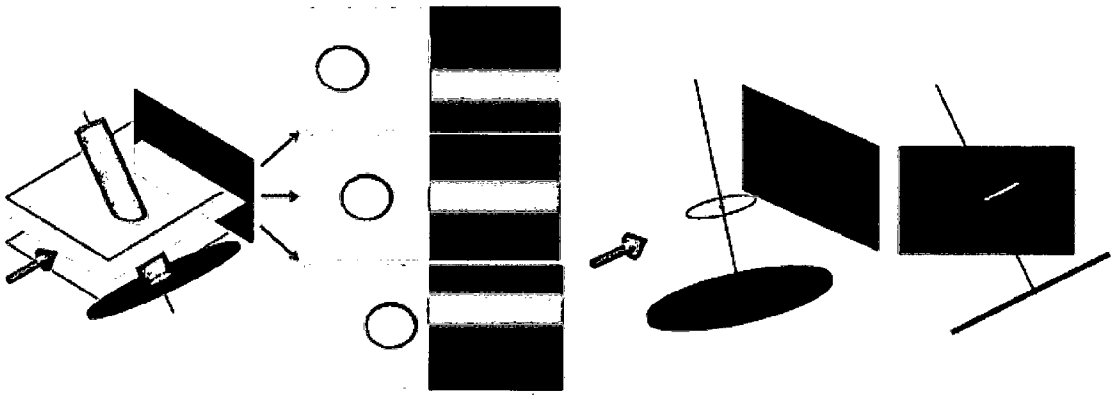

FIG. 8c

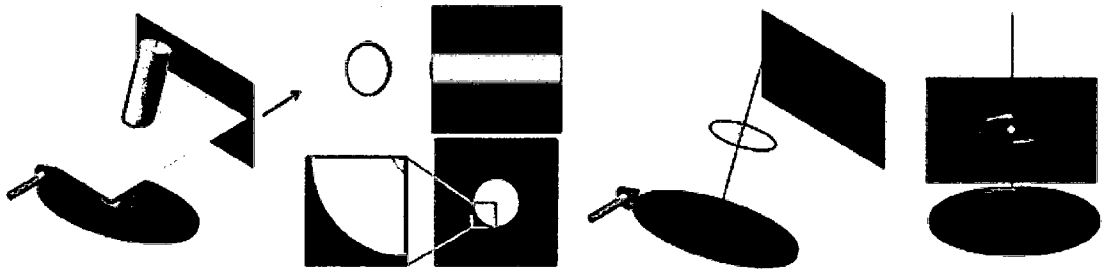

FIG. 9a

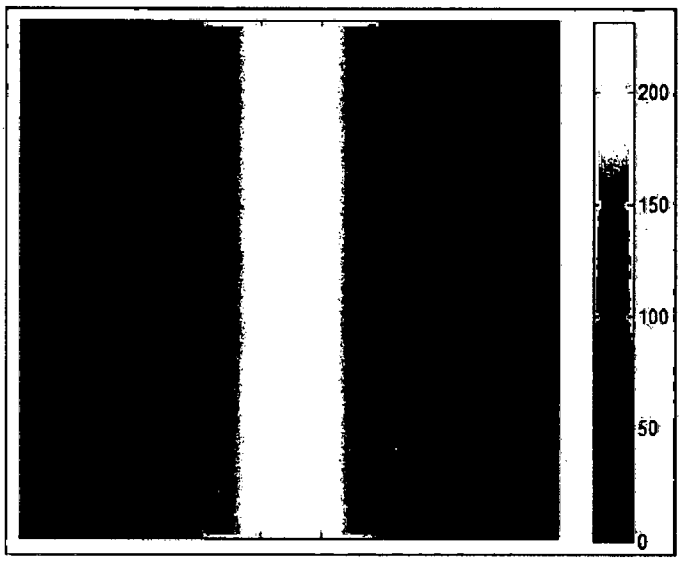

FIG. 9b

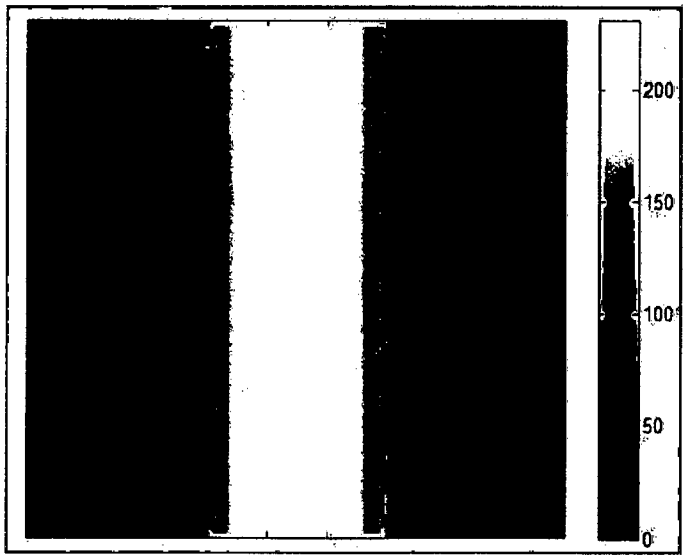

FIG. 9c

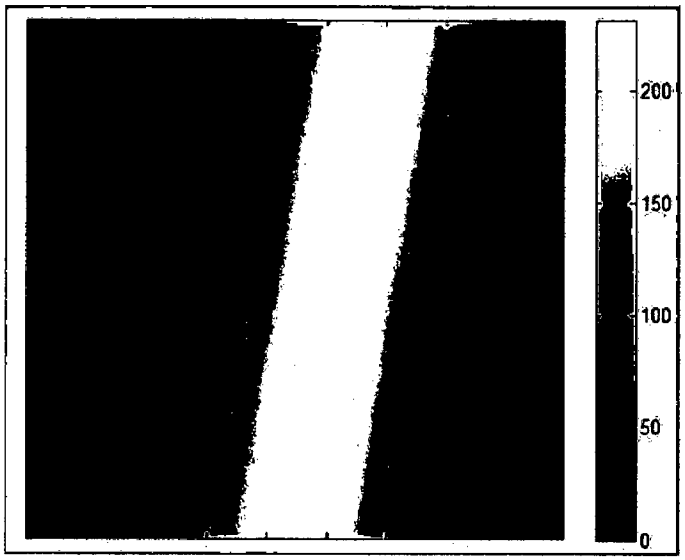

FIG. 10

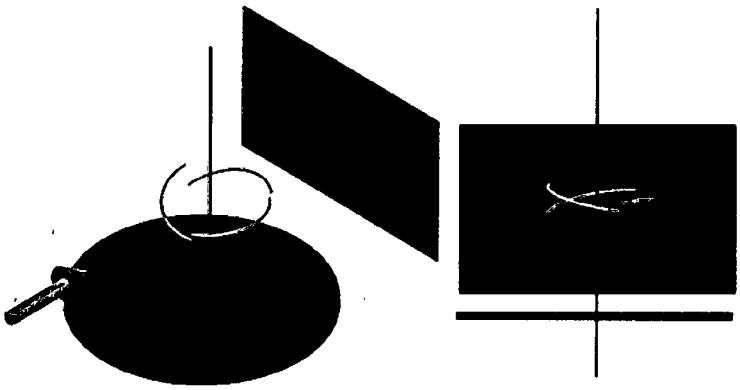

FIG. 11a

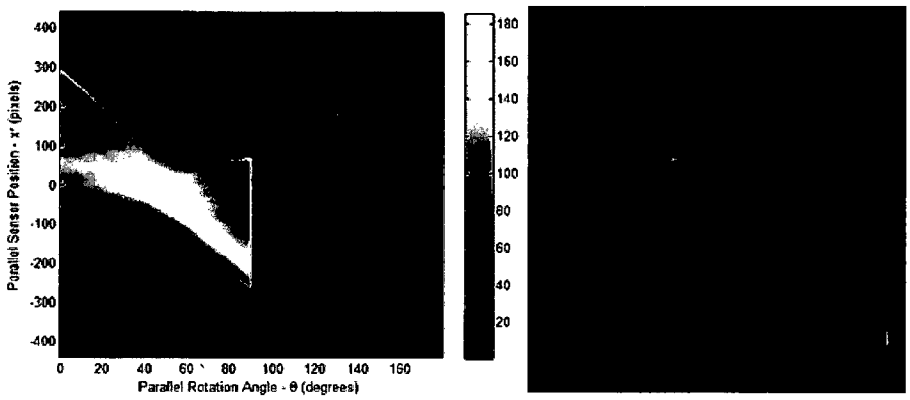

FIG. 11b

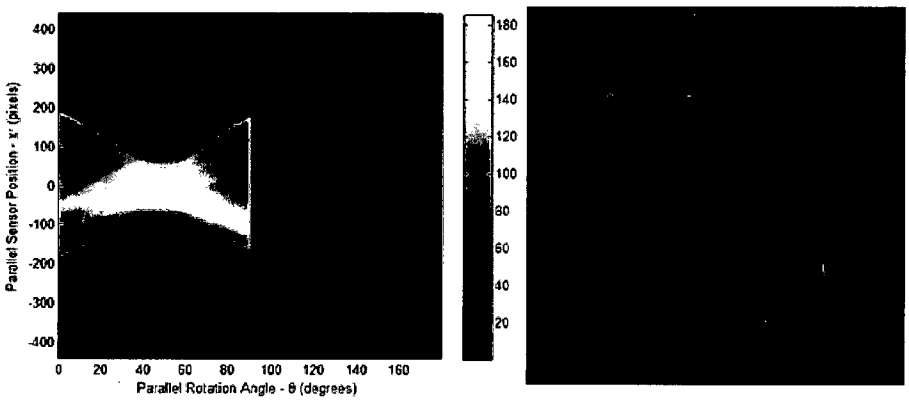

FIG. 12a

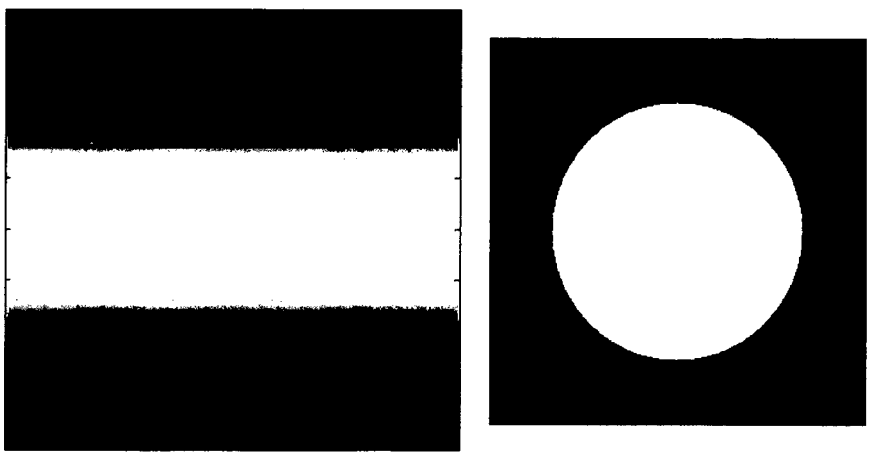

FIG. 12b

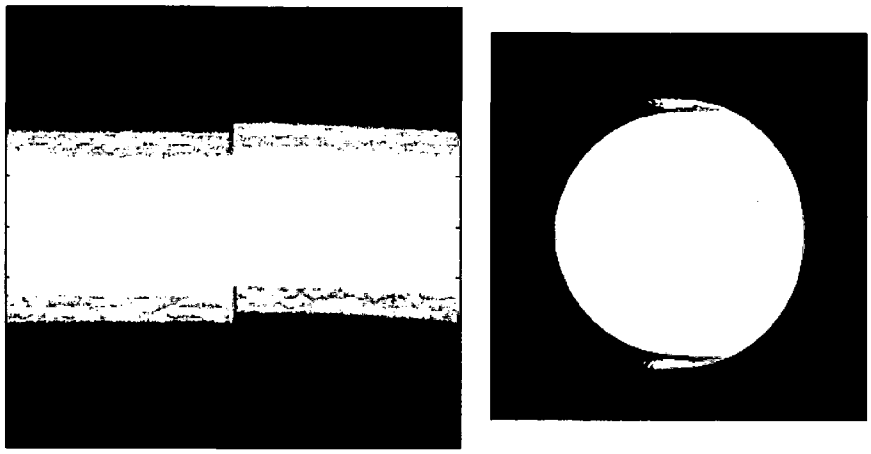

FIG. 12c

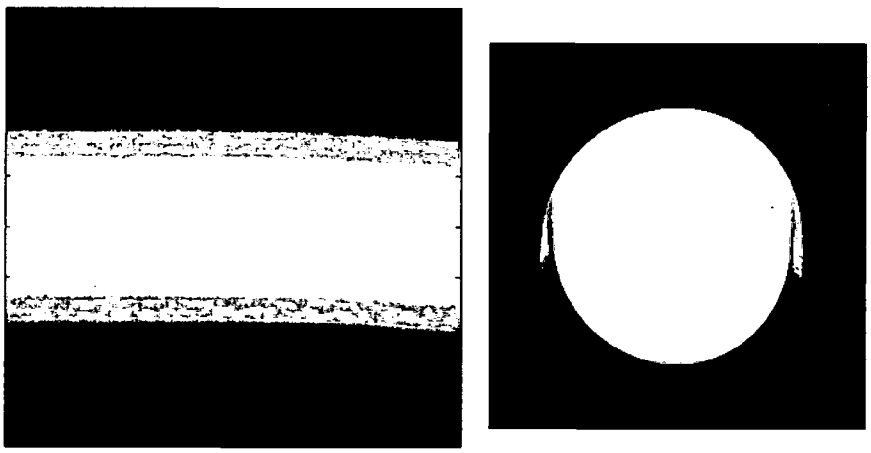

FIG. 13a

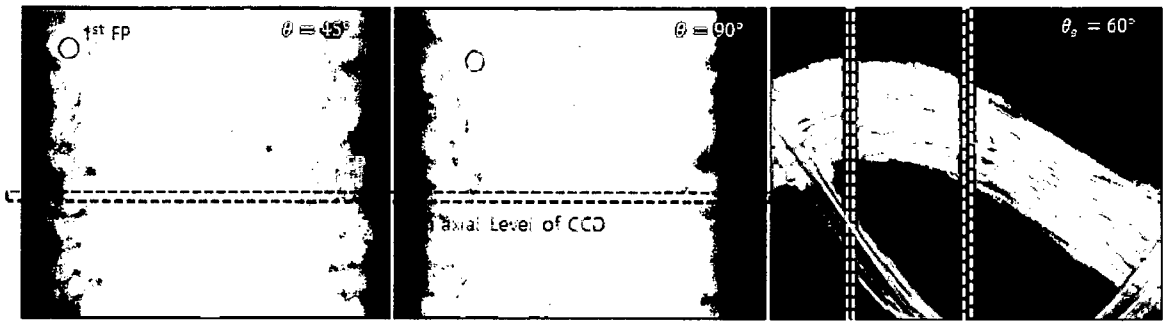

FIG. 13b

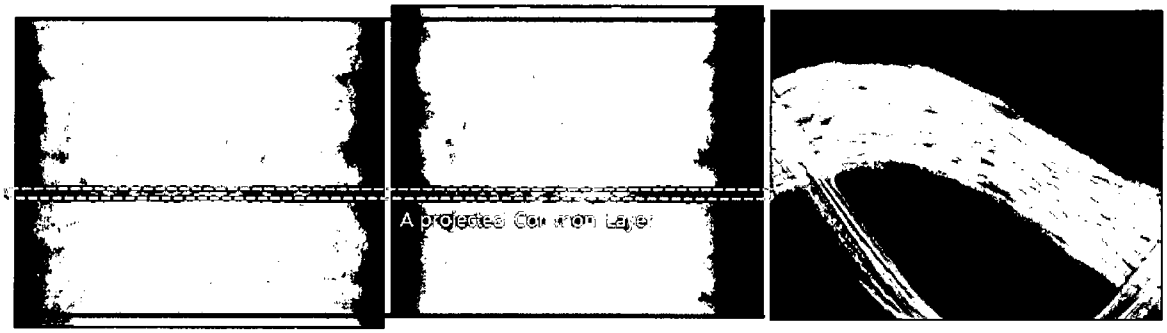

INTERNATIONAL SEARCH REPORT

International application No.
PCT/KR2017/000506

A. CLASSIFICATION OF SUBJECT MATTER

G06T 11/00(2006.01)i, G06T 3/00(2006.01)i

According to International Patent Classification (IPC) or to both national classification and IPC

B. FIELDS SEARCHED

Minimum documentation searched (classification system followed by classification symbols)
G06T 11/00; G01N 23/04; G01T 1/29; G06T 5/00; G06T 3/00

Documentation searched other than minimum documentation to the extent that such documents are included in the fields searched
Korean utility models and applications for utility models
Japanese utility models and applications for utility models

Electronic data base consulted during the international search (name of data base and, where practicable, search terms used)
eKOMPASS(KIPO internal) & Keywords: CT, sinogram, reconstruction, object, line, point, virtual

C. DOCUMENTS CONSIDERED TO BE RELEVANT

Category*	Citation of document, with indication, where appropriate, of the relevant passages	Relevant to claim No.
Y	US 2013-0343508 A1 (GE MEDICAL SYSTEMS GLOBAL TECHNOLOGY COMPANY, LLC) 26 December 2013 See paragraphs [0044]-[0061], [0111]; claims 1, 4-5; and figures 5A-5B, 7.	1-3,7-9,11-15
A		4-6,10
Y	US 9025855 B1 (RALF CHRISTOPH et al.) 05 May 2015 See column 25, line 41-column 26, line 49; claim 10; and figures 14-17.	1-3,7-9,11-15
Y	US 2014-0158890 A1 (STEPHEN PISTORIUS et al.) 12 June 2014 See paragraphs [0028]-[0040]; and figures 1-3.	3,9
A	WO 2015-111052 A1 (YISSUM RESEARCH DEVELOPMENT COMPANY OF THE HEBREW UNIVERSITY OF JERUSALEM LTD.) 30 July 2015 See page 11, line 7-page 14, line 28; and figure 3.	1-15
A	JP 2004-301860 A (TOSHIBA IT & CONTROL SYSTEMS CORP.) 28 October 2004 See paragraphs [0099]-[0108]; and figure 4.	1-15

☐ Further documents are listed in the continuation of Box C.

☒ See patent family annex.

* Special categories of cited documents:
"A" document defining the general state of the art which is not considered to be of particular relevance
"E" earlier application or patent but published on or after the international filing date
"L" document which may throw doubts on priority claim(s) or which is cited to establish the publication date of another citation or other special reason (as specified)
"O" document referring to an oral disclosure, use, exhibition or other means
"P" document published prior to the international filing date but later than the priority date claimed
"T" later document published after the international filing date or priority date and not in conflict with the application but cited to understand the principle or theory underlying the invention
"X" document of particular relevance; the claimed invention cannot be considered novel or cannot be considered to involve an inventive step when the document is taken alone
"Y" document of particular relevance; the claimed invention cannot be considered to involve an inventive step when the document is combined with one or more other such documents,such combination being obvious to a person skilled in the art
"&" document member of the same patent family

Date of the actual completion of the international search	Date of mailing of the international search report
10 April 2017 (10.04.2017)	**11 April 2017 (11.04.2017)**

Name and mailing address of the ISA/KR
International Application Division
Korean Intellectual Property Office
189 Cheongsa-ro, Seo-gu, Daejeon, 35208, Republic of Korea
Facsimile No. +82-42-481-8578

Authorized officer
AHN, Jeong Hwan
Telephone No. +82-42-481-8633

INTERNATIONAL SEARCH REPORT

Information on patent family members

International application No.

PCT/KR2017/000506

Patent document cited in search report	Publication date	Patent family member(s)	Publication date
US 2013-0343508 A1	26/12/2013	JP 2014-000349 A	09/01/2014
		JP 5696963 B2	08/04/2015
		US 9208540 B2	08/12/2015
US 9025855 B1	05/05/2015	CN 102326182 A	18/01/2012
		CN 102326182 B	18/05/2016
		DE 102010000473 A1	26/08/2010
		EP 2399237 A1	28/12/2011
		EP 2399237 B1	14/08/2013
		EP 2654016 A2	23/10/2013
		EP 2654017 A2	23/10/2013
		EP 2654017 A3	07/12/2016
		EP 2665034 A2	20/11/2013
		EP 2665035 A2	20/11/2013
		EP 2665035 A3	07/12/2016
		WO 2010-094774 A2	26/08/2010
US 2014-0158890 A1	12/06/2014	US 2014-0374607 A1	25/12/2014
		US 8866087 B2	21/10/2014
		US 9435901 B2	06/09/2016
		WO 2013-177661 A1	05/12/2013
WO 2015-111052 A1	30/07/2015	EP 3097540 A1	30/11/2016
		US 2016-0335785 A1	17/11/2016
JP 2004-301860 A	28/10/2004	JP 3616928 B2	02/02/2005